

# Strength Evaluation on Interface Weld of Gusset Plate under Pure Tension



**H.ASADA**

*Kobe University, Japan*

**Y.CUI, S.YAMADA**

*Tokyo Institute of Technology, Japan*

**S.KISHIKI**

*Osaka Institute of Technology, Japan*

## SUMMARY:

Braced frames are commonly used lateral-load resisting systems in seismic design. In braced frames, the braces are connected to the beams and columns through gusset plate connection. And fillet welds are commonly used to connect the gusset plate to frame. The ultimate strength of the weld between gusset plate and frame components is determined by the weld effective length, size and stress. There are a few methods that combine various weld effective lengths and stresses are used for design of interface weld of gusset plate connections in Japan. However, applicability of these design methods has not been verified adequately. Experimental study was conducted and showed that it is important to determine the effective length in the estimation of strength and, the Whitmore effective region concept works well. To improve the understanding and design of the ultimate strength of welded gusset plate connections, a series of analytical study was undertaken. The verified numerical model was used to evaluate the ultimate strength of the welded gusset plate connection and interface forces at the gusset-to-beam/column. A parametric study was conducted to examine the influence of the gusset plate size, brace angles, and eccentricity of brace on the connection interface forces. Based on the results, an evaluation of the effective length was suggested.

*Keywords: Steel braced frame, gusset-plate connection, interface weld, ultimate strength, effective length*

## 1. INTRODUCTIONS

Braced frames are widely used for steel constructions in seismic regions. In general, the axial load from the brace is transferred to the beam and column through the gusset plate, which is normally bolted to the brace and connected to the column and beam by welds. Gusset plate should have sufficient strength and stiffness to transfer the applied forces. Failure of the gusset plate connection will result in considerable loss of strength and stiffness of the brace. And the seismic performance of the braced frame is thereby reduced. Among the failure modes of the gusset plate connections, the fracture of the interface weld between the gusset plate and the beam and column is one of the most undesirable failure modes(Astaneh-Asl, 1988),(Roeder, et al., 2005). However, few studies have done yet on the ultimate behavior of the gusset plate connection when the fracture of interface welds occurred. In US, the interface weld is commonly designed by the Uniform Force Method (UFM)(Thornton, 1991),(AISC, 2005) as recommended by AISC. In Japan, there are various design practices for the interface weld. However, the adequacy of the methods of design with respect to safety and economy of construction has not been confirmed. On the other hand, fillet welds are commonly used to connect the gusset plate to the beam and column due to the overall economy and ease of fabricating. The fillet welds exhibited less desirable behavior than the complete joint penetration (CJP) groove welds as discussed in previous studies(Lehman, et al., 2008),(Yoo, et al.,2008). The tapered gusset plates are commonly used in the conventional braced frames in Japan. Compared with the rectangular gusset plate, the resistance capacity of the interface weld of the tapered gusset plate is more critical. A unified design method of the interface weld, which could provide the safe and economical design, is needed. In Japan, three design methods (AIJ, 2012),(BCJ, 2007),(JSSC, 2009) of the gusset plate connections interface weld are commonly used. The differences between the three

design methods are the effective length of the interface weld and the orientation of the resultant force on the interface weld. The previous experimental research (Asada, et al., 2010) indicated that the method recommended by Architectural Institute of Japan (AIJ method)(AIJ, 2012) gave the better evaluation on the ultimate strength of the gusset plate when the interface weld fractured. It is primarily because the effective length of interface weld within the 30-degree effective region was considered in AIJ method. However, further data are required to evaluate the workability of the design method. This paper attempts to seek a unified design method. This study focuses on the ultimate behavior of the gusset plate connection with fillet welds. The axial force transferred by the gusset plate when the interface weld fractured is termed as the ultimate strength of the gusset plate connection here. The effect of the gusset plate size, brace angle, and eccentricity of brace on the ultimate strength of the gusset plate connection was discussed using the finite element model. Based on the analytical results, one of the current design methods in Japan is recommended and revised by considering the effect of geometry size of gusset plate.

**2. NUMERICAL MODELING**

In previous study (Cui, et al., 2011), A comprehensive series of nonlinear, inelastic FE analyses were performed to simulate the response of the test specimens using the ABAQUS 6.9, and it was confirmed that previous test results (Asada, et al., 2011) conducted by authors can be simulated by using the following numerical model. Fig. 1 shows a typical FE model of a gusset plate connection specimen. The gusset plate at the intersection between the beam and the column was partitioned into 5 mm height slice to represent the weld. The FE model was constructed using 3D solid element for all components. 8-node linear brick, reduced integration element was used for the gusset plate and two endplates. The equivalent region of weld on the gusset plate was modelled by 8-node linear brick element. A mesh refinement study was conducted to determine the mesh size required to ensure convergence and accuracy of the FE solution and simultaneously minimizing the execution time. On the basis of this study, a fine mesh (5 mm) was used for the gusset plate, and finer mesh (1.25 mm) was used for the weld part. Elastic-plastic and strain hardening material models were used for the gusset plate. Elastic-plastic material with a maximum stress of 575 N/mm<sup>2</sup> and stress reduction to 100 N/mm<sup>2</sup> at strain of 0.1 was assigned to the weld region on the gusset plate, as shown in Fig.1 (b). The weld fracture is predicted by considering the strain at the weld part is over 0.1. The translational degrees of freedom at the nodes along the bolt holes of the two endplates were fully restrained. The load was applied through the nodes along the front half side bolt holes considering the bearing interaction between bolts and gusset plate during the loading. Monotonic in-plane displacement was loaded along the brace direction in tension, as shown in Fig. 1 (c).

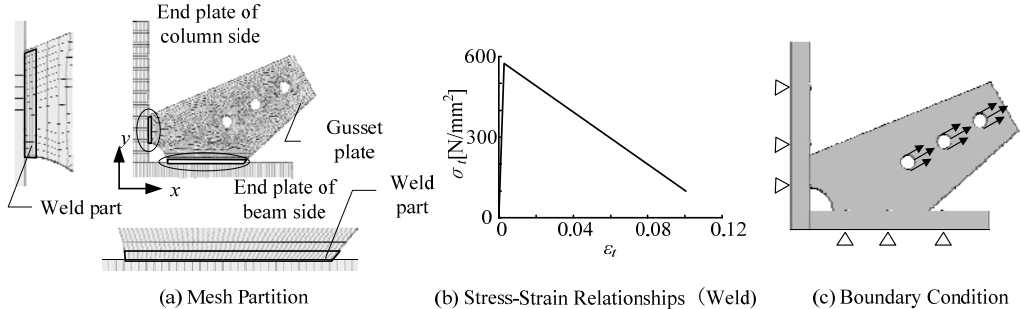


**Figure 1.** FE model

**3. PARAMETRIC ANALYSIS**

**3.1 Overview of Parametric Study**

The FE analytical models discussed above were used to extend the prior studies to examine a range of parameters that were not evaluated in the experimental research program. To avoid gusset plate fracture, the elastic material property was assigned to the gusset plate. The results aid in investigating the stress distribution of the interface weld and resultant force distribution of the gusset plate

connection with a broader range of geometries. The studied design parameters include the geometry of the gusset plate ( $L_x, L_y$ ), brace angle ( $\theta$ ), and eccentricity of the brace along the beam side ( $e_x$ ). The definition of the parameters is shown in Fig. 2.

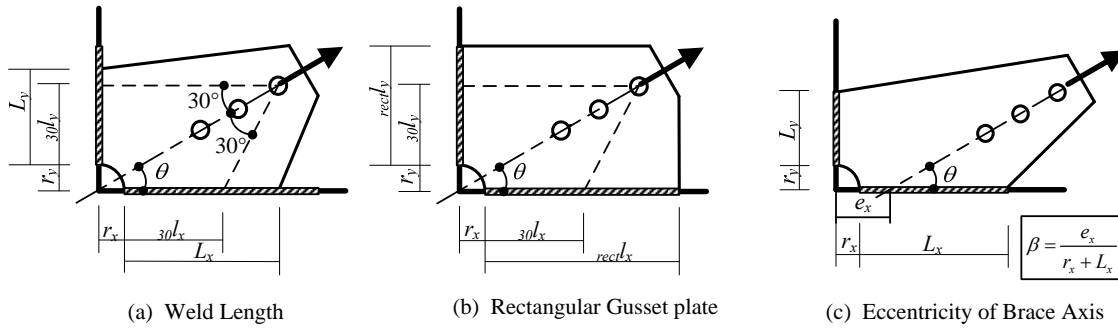


**Figure 2.** Gusset plate geometries

The values of each parameter are described below. To be noticed, the end returns of the fillet weld was used for the specimens in this study. Therefore, it is not necessary to subtract two times the nominal fillet weld size to count the weld length. The gusset plate size was varied based on the 30-degrees effective region (AIJ, 2012) and the rectangular shape, as shown in Fig. 2(b). Four types of interface weld length were chosen for beam and column side, respectively. They are half the 30-degrees effective length ( $0.5 \cdot 30l$ ), the 30-degrees effective length ( $30l$ ), the length between 30-degrees effective length and rectangular length ( $0.5 \cdot (30l + rectx)$ ), and the rectangular length ( $rectx$ ). Brace angle was 30 and 45 degrees. Eccentricity along beam side is controlled by the offset ratio  $\beta$  (see Eq. (3.1)), as shown in Fig.1(c). In this study, the offset ratios of 0.25 and 0.33 were used.

$$\beta = \frac{e_x}{r_x + L_x} \quad (3.1)$$

where,  $r_x$  is the size of the weld access hole on beam side,  $e_x$  is the offset distance of the brace along the beam side. The parameters groupings and specific values for individual specimens that were analysed within each group are identified in Table 1 (shaded cells indicate the prototype models for the models with brace eccentricity). As the designation of the experimental specimen, the designation of each simulation model indicates the studies parameter and its value. For the specimens with brace eccentricity, specimen B135-C90-033E indicates the gusset plate B135-C90 with the brace offset ratio of 0.33, the name in brackets indicates the size of the gusset plate. There are 16 analyzed models with the brace angle of 30 degrees and 10 models with the brace angle of 45 degrees when the brace axis pass through the corner of the gusset plate. Also, there are 16 models for the eccentric gusset plate connections.

**Table 1.** List of models

(a) $\theta=30^\circ$ , No eccentricity					(b) $\theta=45^\circ$ , No eccentricity				
Ly [mm]	Lx[mm]				Ly [mm]	Lx[mm]			
	60	135	200	265		60	108	165	217
45	B60-C45	B135-C45	B200-C45	B265-C45	60	B60-C60	B108-C60	B165-C60	B217-C60
90	B60-C90	B135-C90	B200-C90	B265-C90	108	-	B108-C108	B165-C108	B217-C108
120	B60-C120	B135-C120	B200-C120	B265-C120	165	-	-	B165-C165	B217-C165
150	B60-C150	B135-C150	B200-C150	B265-C150	217	-	-	-	B217-C217

(a) $\theta=30^\circ$ , Eccentricity			(b) $\theta=45^\circ$ , Eccentricity		
$\beta$	0.25	0.33	$\beta$	0.25	0.33
B60-C60	B60-C45-025E (B92-C45)	B60-C45-033E (B105-C45)	B60-C60	B60-C60-025E (B92-C60)	B60-C60-033E (B150-C60)
B135-C90	B135-C90-025E (B190-C90)	B135-C90-033E (B220-C90)	B108-C108	B108-C108-025E (B155-C108)	B108-C108-033E (B220-C90)
B200-C120	B200-C120-025E (B280-C120)	B200-C120-033E (B315-C120)	B165-C165	B165-C165-025E (B230-C120)	B165-C165-033E (B265-C120)
B265-C150	B265-C150-025E (B365-C150)	B265-C150-033E (B410-C150)	B217-C217	B217-C217-025E (B300-C217)	B217-C217-033E (B340-C217)

### 3.2 Interface Stress Distribution

Typical von-Mises stress distributions along interface weld at the ultimate strengths of the gusset plate connections are shown in Fig. 3, in which the dash line shows the AIJ effective length (AIJL). The shape and size of each specimen and the 30-degree effective regions are also shown. Figure 5 (a) and (b) show the von-Mises stress distribution of the interface weld of analytical specimens B135-C45 and B108-C108, in which gusset plates are within the 30-degree effective region. To be noted that the von-Mises stress distributions are uniform and the entire interface weld of both specimens reach the maximum weld stress (575MPa) on both the beam and column side. For the analytical specimen B217-C217, in which the gusset plate is larger than the 30-degree effective region, the von-Mises stress distribution was uniform and the von-Mises stress reached the maximum weld stress within the 30-degree effective region. The von-Mises stress reduced gradually along the interface weld at the portion out of the 30-degree effective region. Fig. 3 (d) compares the von-Mises stress distribution of the analytical specimen B135-C90, in which the interface weld length of the column side increased from 45 mm to 90 mm to the one of the specimen B135-C45 (Fig. 3 (a)). In this specimen, the entire interface weld reached the maximum stress on the beam side, while only a part of the interface weld on the column side reached the maximum stress. The same behavior was observed for the analytical specimen B108-C60 (Fig. 3 (e)), in which the column side interface weld length reduced from 108 mm to 60mm by comparison with the specimen B108-C108 (Fig. 3 (b)). The stress distribution of the analytical specimen B217-C217-033E (B300-C217), in which the brace axis is offset by 121 mm from the gusset plate corner, is shown in Fig. 3 (f). It is noted the interface weld within the 30-degree effective region on the beam side reached the maximum stress. However, the interface weld stress was relatively small on the column side; even the interface weld of the column side is longer than the AIJ effective length. As observed from the analytical results, the interface weld within the 30-degree effective region generally reached the maximum weld stress at the ultimate strength of the gusset plate connection. However, the stress distribution of the interface weld was also affected by the gusset plate size, brace angle, and eccentricity of the brace.

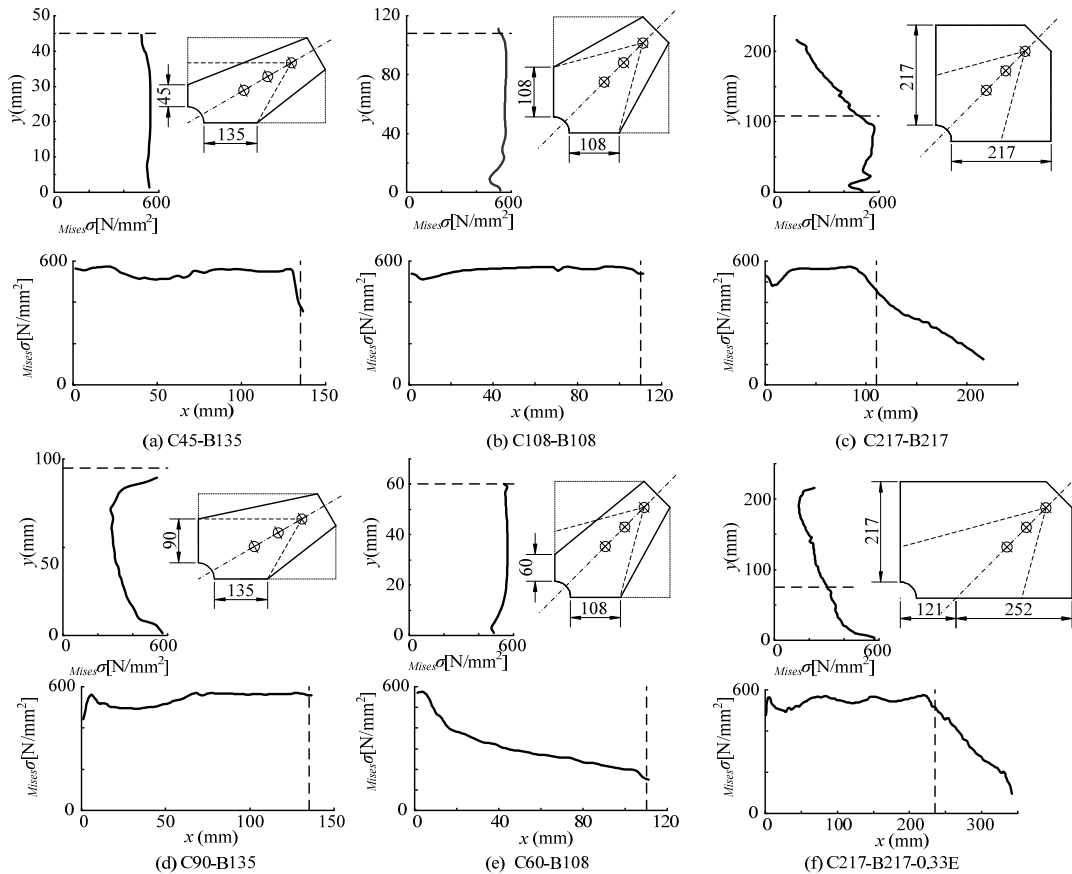


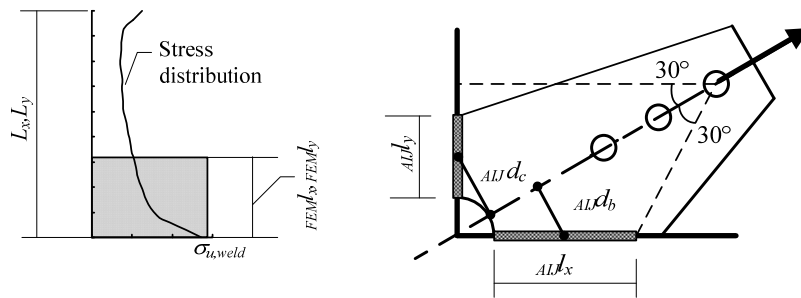
Figure 3. Stress distribution along interface weld

### 3.3 Effective Length

To quantify the resistance region of the interface weld, the effective length ( ${}_{FEM}l$ ) is calculated based on the von-Mises stress distribution discussed in previous section using Eq. 2. As illustrated in Fig. 4, the weld stress is assumed to reach the ultimate stress and uniformly distributed along the interface weld within the effective length ( ${}_{FEM}l$ ).

$${}_{FEM}l = \sum \sigma_i \cdot l_i / \sigma_{u,weld} \quad (3.2)$$

Where,  ${}_{FEM}l$  is the effective length calculated from the analytical results,  $l_i$  is the distance between each measured node,  $\sigma_i$  is the von-Mises stress at the measured node,  $\sigma_{u,weld}$  ( $=575\text{MPa}$ ) is the maximum weld stress. Fig. 5 shows the AIJ effective length ( ${}_{AIJ}l_x, {}_{AIJ}l_y$ ) and the distance from the centroid of the AIJ effective length to the brace axis ( ${}_{AIJ}d_B, {}_{AIJ}d_C$ ). The effective lengths evaluated based on the numerical results ( ${}_{FEM}l$ ) are compared with the AIJ effective length ( ${}_{AIJ}l$ ) in Fig. 6. The ratio of  ${}_{FEM}l/{}_{AIJ}l$  is larger than 1.0 indicates that the effective length is underestimated by AIJ effective length, while if the ratio is smaller than 1.0, the effective length is overestimated by AIJ effective length. The ratio of the distance from the centroid of the AIJ effective length on the beam and column side to the brace axis ( ${}_{AIJ}d_B/{}_{AIJ}d_C$ ) is shown in Fig. 7, too. When the gusset plate is within 30-degree effective region, the AIJ effective length could evaluate the effective length of interface weld well for the brace without eccentricity. The effective length of interface weld on beam side is overestimated by AIJ effective length ( ${}_{FEM}l_x/{}_{AIJ}l_x < 1.0$ ) when the distance from interface weld on beam side to brace axis is larger than the distance from interface weld on column side ( ${}_{AIJ}d_B/{}_{AIJ}d_C > 1.0$ ). And the effective length of interface weld on column side is overestimated by AIJ effective length ( ${}_{FEM}l_y/{}_{AIJ}l_y < 1.0$ ) when the distance from interface weld on column side to brace axis is larger than the distance from interface weld on beam side ( ${}_{AIJ}d_B/{}_{AIJ}d_C < 1.0$ ). The same tendency for the effective length of interface weld was observed for the specimens with eccentric brace connection. When the gusset plate is larger than 30-degree effective region, the AIJ effective length ( ${}_{AIJ}l$ ) tended to underestimate the effective length. This is primarily because the contribution of the stress distributed beyond the 30-degree effective region, as shown in Fig. 3(c) and (f), is not taken into account by AIJ effective length. As the brace eccentricity along the beam side increased, the effective length of interface weld on beam side could be evaluated by the AIJ effective length with a reasonable difference. For the gusset plate with the brace angle of 30 degree, the effective length on column side was further overestimated by the AIJ effective length as the brace eccentricity increased. For the brace angle of 45 degree, the effective length on column side could be evaluated well by the AIJ effective length with the eccentricity of brace. As discussed above, the AIJ effective length is able to evaluate the effective length reasonably when the brace angle is 45 degrees and the gusset plate is within the 30-degree effective region. However, it is not able to consider the interaction of the gusset plate size, brace angle, and eccentricity of the brace. The AIJ effective length to consider such interaction using the relative distance from interface weld of each side to brace axis is suggested.



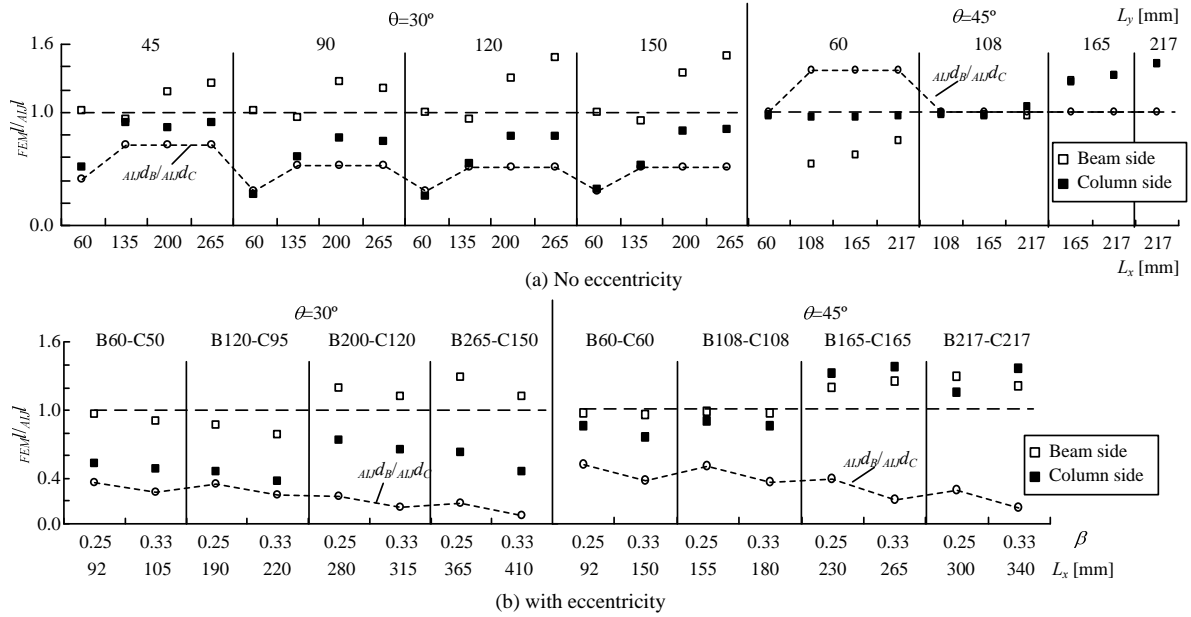


Figure 6. Comparison of FEM effective length with AIJ effective length

## 4. EVALUATION OF RESULTANT FORCE OF INTERFACE WELD

### 4.1 Hypothesis of Evaluation

#### (a) Resultant force angle

The horizontal and vertical resultant force components of the interface weld are used to calculate the resultant force angle on the beam and column side ( $\theta_B$  and  $\theta_C$ ), respectively, as illustrated in Fig. 7 (a). Figure 8 shows the resultant force angle of the beam and column side at the ultimate strength of the gusset plate connection for each analytical specimen. It's noted that the resultant force is generally aligned to the brace axial. A similar observation was also made in the previous study (Richard). The resultant force angle tends to be larger when the size of the gusset plate is larger than the 30-degree effective region. However, the variation is relatively small. This observation explains why the AIJ method, in which the resultant force on the interface weld is assumed parallel to the brace, worked well among the three methods of Japanese design methods

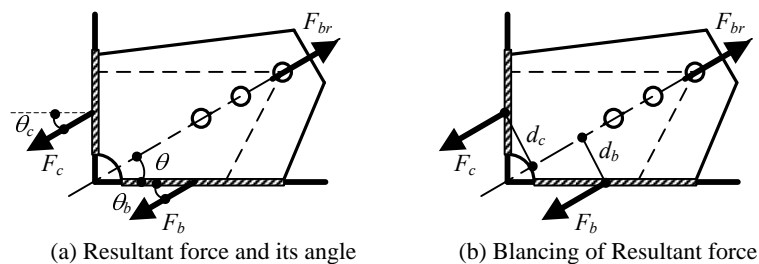


Figure 7. Resultant Force on column and beam side

#### (b) Resultant force distribution

To design the gusset plate connection, an estimate of the resultant force distribution is required. As shown in Fig. 7(b), the transferred brace force  $F_{br}$  is resisted by the resultant forces on the beam and column side,  $F_B$  and  $F_C$ . Taking moments about the corner of the gusset plate,

$$\begin{aligned} F_B &= F_{br} \cdot_{FEM,e} d_c / (_{FEM,e} d_B + _{FEM,e} d_c) \\ F_C &= F_{br} \cdot_{FEM,e} d_b / (_{FEM,e} d_B + _{FEM,e} d_c) \end{aligned} \quad (4.1)$$

where,  $_{FEM,e} d_B$  is the distance from the centroid of the effective interface weld measured from

numerical results on the beam side to the brace axis, while,  ${}_{FEM,e}d_C$  is the distance from the column side, as illustrated in Fig.7(b).The calculated resultant force using Eq. 3 ( $F_B$  and  $F_C$ ) is compared with the resultant force from the analytical results ( ${}_{FEM}F_B$  and  ${}_{FEM}F_C$ ) in Fig. 9. The calculated resultant force and the analytical results differ within a range of 20% in the case of the majority of the analytical specimens. The large difference was observed when the gusset plate size presents extremely asymmetry (e.g., specimens B200-C45 and B265-C45).

#### 4.2 Revised AIJ Effective Length

As discussed previously, it is necessary to evaluate the effective length for the evaluation of the ultimate strength of the gusset plate connection. Here, the AIJ effective length is revised by considering the distance from the interface weld of each side to the brace axis. Considering the geometry configuration, the relation between the effective length ( $eL_x, eL_y$ ) and the distance to the brace axis ( $d_B, d_C$ ) was as follows

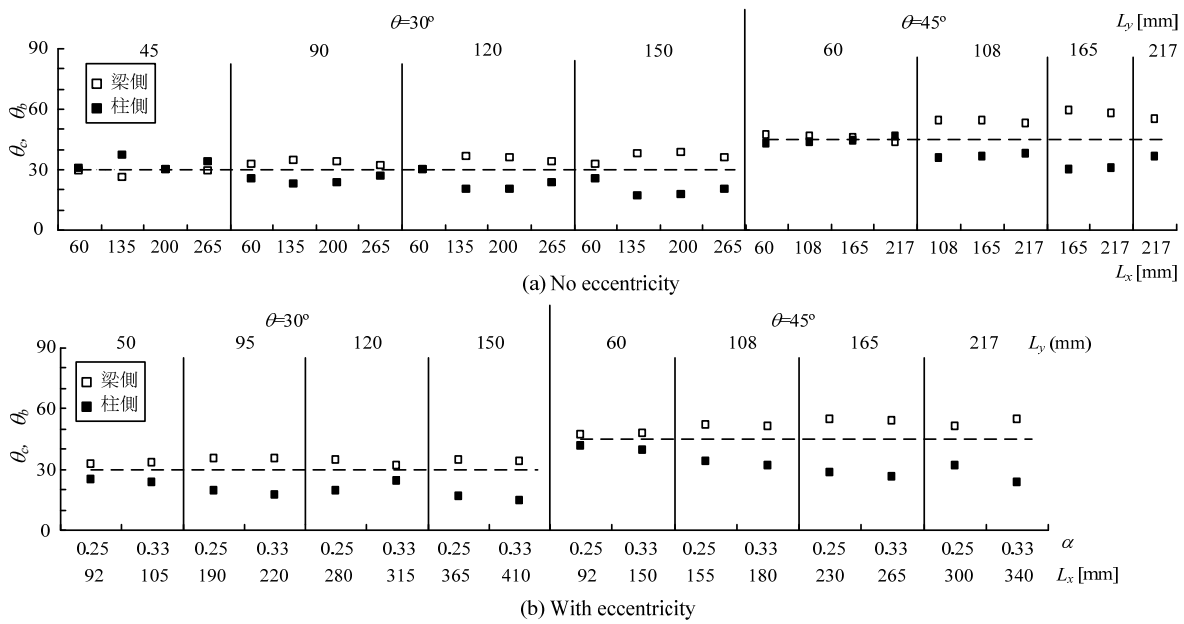


Figure 8. Resultant force angles on column and beam side obtained from FEM results

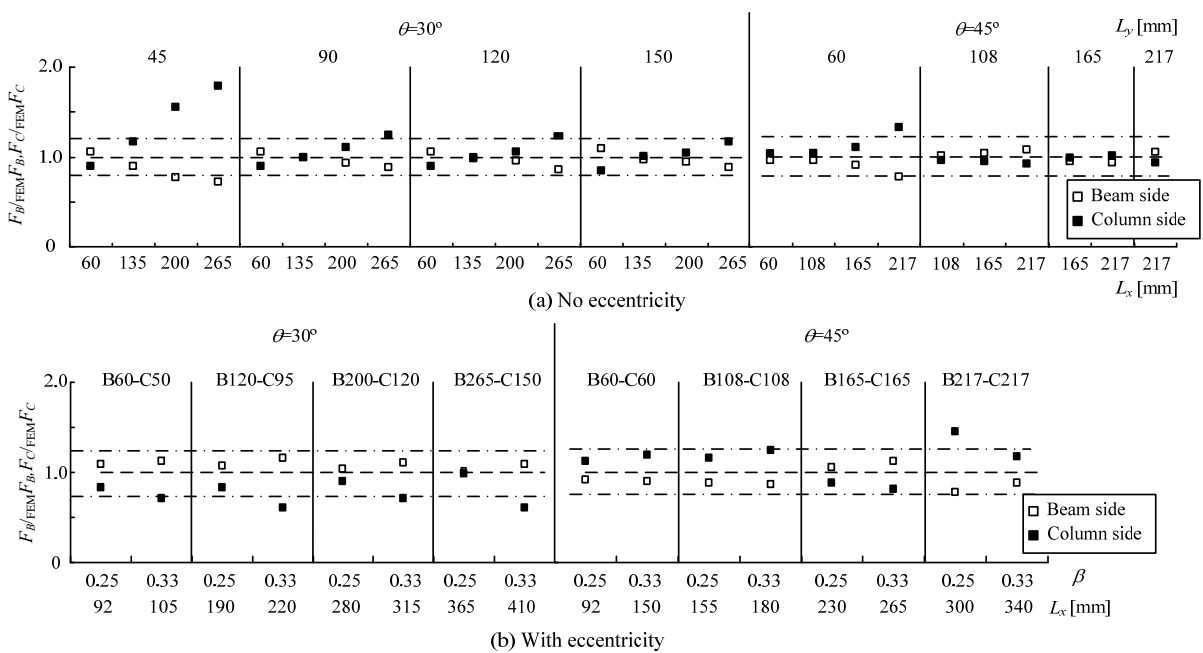


Figure 9. Comparison of resultant force from numerical results and calculated by using Eq.(4.1)

$$\begin{aligned}d_B &= (e l_x / 2 + r_x - e_x) \sin \theta \\d_C &= (e l_x / 2 + r_x + e_x \tan \theta) \cos \theta\end{aligned}\quad (4.2)$$

On the other hand, the relation also followed the static equilibrium conditions. Based on the observation of the parametric study, it was assumed that the resultant force on the interface weld is aligned with the brace. The plane stress condition was adopted to describe the interface weld stress statement. Horizontal and vertical force equilibrium gives:

$$\begin{aligned}F_{VB} &= F_B \sin \theta, F_{HB} = F_B \cos \theta \\F_{HC} &= F_C \sin \theta, F_{CC} = F_C \cos \theta\end{aligned}\quad (4.3a,b)$$

The von-Mises stress of the interface weld was used to predict the failure

$$\sigma_{u,weld} = \sqrt{\sigma_i^2 + 3\tau_i^2}, i = B, C \quad (4.4)$$

in which,

$$\begin{aligned}\sigma_B &= F_{VB} / (t_p \cdot e l_x), \tau_B = F_{HB} / (t_p \cdot e l_x) \\ \sigma_C &= F_{VC} / (t_p \cdot e l_y), \tau_C = F_{HC} / (t_p \cdot e l_y)\end{aligned}\quad (4.5a,b)$$

where,  $e l_x$  is the effective length on the beam side [mm],  $e l_y$  is effective length on the column side [mm], and  $t_p$  is the thickness of gusset plate [mm].

Solving Eqs. (4.3), (4.4), and (4.5) simultaneously gives

$$\begin{aligned}{}_{u,w}F_B &= \sigma_u \cdot t_p \cdot e l_x / \sqrt{\sin^2 \theta + 3 \cos^2 \theta} \\ {}_{u,w}F_C &= \sigma_u \cdot t_p \cdot e l_y / \sqrt{\cos^2 \theta + 3 \sin^2 \theta}\end{aligned}\quad (4.6a,b)$$

where,  ${}_{u,w}F_B$  and  ${}_{u,w}F_C$  are the ultimate strength of interface weld on beam and column side [kN], respectively. Therefore, the relation between the effective length ( $e l_x, e l_y$ ) and the distance to the brace axis ( $d_B, d_C$ ) is

$$e l_x / e l_y = d_C / d_B = \sqrt{\sin^2 \theta + 3 \cos^2 \theta} / \sqrt{\cos^2 \theta + 3 \sin^2 \theta} \quad (4.7)$$

The AIJ effective length is revised by considering the balancing of the interface weld of the beam and column side. The procedure for balancing the interface welds of the beam and column side may be summarized as follows:

1. Compute the AIJ effective length,  ${}_{AIJ}l_{x,y}$ , and the distance from the center of this effective length to the brace axis,  ${}_{AIJ}d_{B,C}$ .
2. Identify the critical side that controls the effective length by comparing  ${}_{AIJ}d_B$  and  ${}_{AIJ}d_C$ .  
if  ${}_{AIJ}d_B > {}_{AIJ}d_C$ ,  $e l_y = {}_{AIJ}l_y$   
if  ${}_{AIJ}d_B < {}_{AIJ}d_C$ ,  $e l_x = {}_{AIJ}l_x$   
if  ${}_{AIJ}d_B = {}_{AIJ}d_C$ ,  $e l_x = {}_{AIJ}l_x$  and  $e l_y = {}_{AIJ}l_y$
3. Compute the other side effective length using Eqs. 4.4 and 4.8, which is

$$\begin{aligned}e l_x &= (e_x - r_x) + \sqrt{(e_x - r_x)^2 + [e l_y^2 + 2(r_y + e_x \tan \theta) \cdot e l_y]} / \alpha \\ e l_x &= -(r_x + e_x \tan \theta) + \sqrt{(r_y + e_x \tan \theta)^2 + [e l_x^2 + 2(r_x - e_x) \cdot e l_x]} / \alpha\end{aligned}\quad (4.8a,b)$$

in which,

$$\alpha = \tan \theta \cdot \sqrt{(\cos^2 \theta + 3 \sin^2 \theta)} / \sqrt{\sin^2 \theta + 3 \cos^2 \theta} \quad (4.9)$$

The calculated effective lengths ( $e l_{x,y}$ ) are compared with the effective length measured from numerical

results ( $FEM l_{x,y}$ ) in Fig.10. The calculated effective length agreed with numerical effective length well when the gusset plate is compact. When the gusset plate is larger or the eccentricity of the brace is larger, the proposed evaluation tends to underestimate the effective length.

#### 4.3 Evaluation of the Ultimate Strength of Gusset Plate Connection

With the revised effective length, the ultimate strength of the gusset plate connection ( ${}_{u,w}F_{br}$ ) is calculated using Eq. (4.10).

$${}_{u,w}F_{br} = {}_{u,w}F_B + {}_{u,w}F_C \quad (4.10)$$

The calculated ultimate strengths of the gusset plate connections were compared with the ones from the FE analyses for each analytical specimen in Fig. 11. Three types of length were used to calculate the ultimate strength. They are the revised AIJ effective length ( ${}_e l_{x,y}$ ), the AIJ effective length ( ${}_{AIJ} l_{x,y}$ ), and the entire length ( $L_{x,y}$ ). It is noted that using the revised AIJ effective length ( ${}_e l_{x,y}$ ), the calculated ultimate strengths of the gusset plate connection are continually conservative. The difference between calculation and FEM results is within 20% for the gusset plate is not greater than the 30-degree effective region. When the gusset plate is larger than the 30-degrees effective region, the error was increased from 20% to 70%, since the resistance stress of the interface weld beyond the 30-degrees effective region was not taken into account in the revised AIJ effective length. However, a degree of conservatism in the design of the gusset plate connection may be warranted for the whole braced frame performance. For the comparison, the calculated ultimate strengths using the entire interface weld length ( $L_{x,y}$ ) and the AIJ effective length ( ${}_{AIJ} l_{x,y}$ ) are larger value than that observed from the numerical study, specifically when the brace angle is 30 degrees. It is primarily because the effective region of the interface weld was not reasonably represented by either the entire length or the AIJ effective length.

### 5. CONCLUSIONS

This paper attempts to seek a unified design method of the interface weld of gusset plate connection with fillet weld with the tension brace. The finite element models verified with the previous experimental study were adopted for the further parametric study to investigate the effect of the gusset plate size, brace angle, and eccentricity of the brace on the resistance strength of the interface weld. Based on the parametric study, the following were observed. The interface weld within the 30-degrees effective region transfers almost all the brace force from the gusset plate to the beams and columns. The effective interface length is affected by the gusset plate size, brace angle, and eccentricity of the brace. The resistance force of the interface weld is generally aligned to the brace. Based on the pre-mentioned observations, the AIJ 30-degrees effective length was modified by considering the geometrical effect of the gusset plate (such as, the gusset plate size, brace angle, and eccentricity of brace). The revised evaluations of the interface weld were presented. The evaluation of the resistance strength of the interface weld with the revised AIJ 30-degrees effective length was constantly conservative in comparison with that with the original AIJ 30-degrees effective length and the entire length.

### REFERENCES

- Astaneh-Asl H. (1998). Seismic Behavior and Design of Gusset Plates. Steel Tips, Moraga Calif.: Structural Steel Education Council
- Roeder C, Lehman D, Yoo, JH. (2005). Improved Seismic Design of Steel Frame Connections, International Journal of Steel Structures, Vol. 5, 141-153
- Thornton WA.(1991). On the Analysis and Design of Bracing Connections., Proc. of national steel construction conference, Washington. DC, AISC, 26-33
- AISC (2005). Steel Construction Manual. 13th ed. Chicago (IL), American Institute of Steel Construction
- Lehman D, Roeder C, Herman D, Johnson S, Kotulka B. (2008). Improved Seismic Performance of Gusset Plate Connection, Journal of Structural Engineering (ASCE), Vol. 134(6), 890-901

Yoo JH, Roeder CW, Lehman DE. (2008). Analytical Performance Simulation of Special Concentrically Braced Frames, *Journal of Structural Engineering (ASCE)*, Vol. 134(6), 881-889

AIJ (2012). Recommendations for Design of Connections in Steel Structures, Architectural Institute of Japan, Tokyo

The Building Center of Japan (BCJ). (2007) Commentary of Structure Design Provisions for Buildings 2007, Government Publications Service Center, Tokyo

Japanese Society of Steel Construction (JSSC). (2009) Fundamentals of Steel Structure Design. 4th ed., Gihodoshuppan, Tokyo

Asada H, Yamada S, Kishiki S, Minowada S.(2011). Investigation of Tension Brace Connections in Existing Steel Gymnasium and Evaluation on Ultimate Strength of Fillet Welded Gusset Plate Connection. *J. Struct. Constr. Eng. (Transactions of AIJ)*, Vol. 76, No. 659, 185-193

ABAQUS.(2009). ABAQUS/ Standard User's Manual. Version 6.9. Hibbit, Karlson and Sorensen, Inc.

Cui, Y, Asada,H., Kishiki, S., Yamada, S., (2011). Strength Evaluation of Gusset Plate Connections with Fillet Weld , Part II Parametric Study, Proceedings of Kanto Branch Annual Meeting, Tokyo, AIJ, 169-172,

Richard R., Analysis of Large Bracing Connection Designs for Heavy Construction. Proceedings

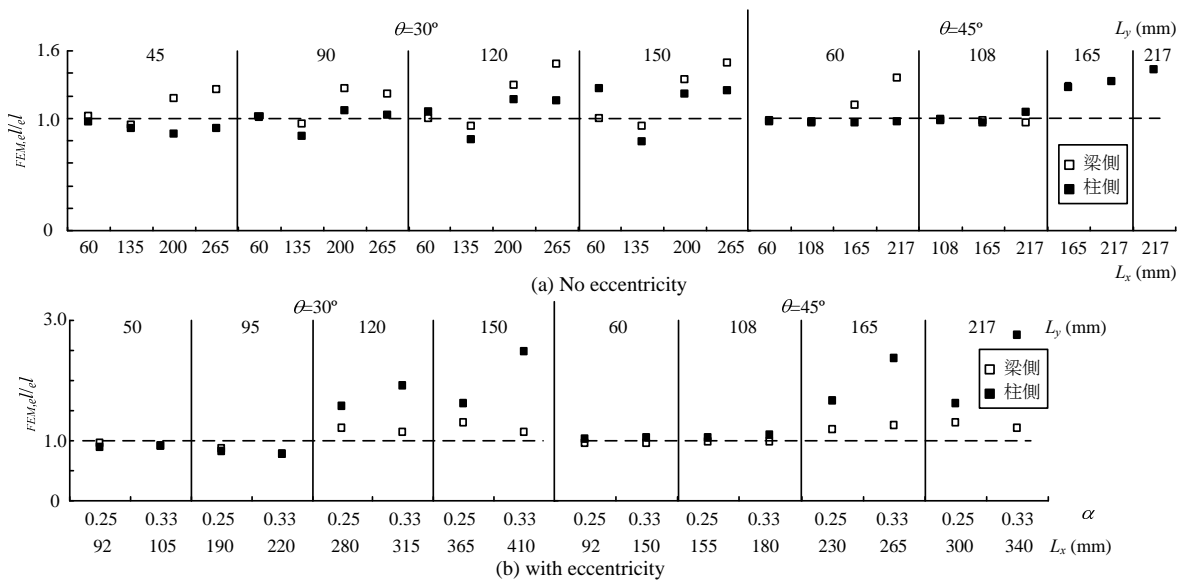


Figure 10. Comparison of effective length from numerical and calculated by proposed method

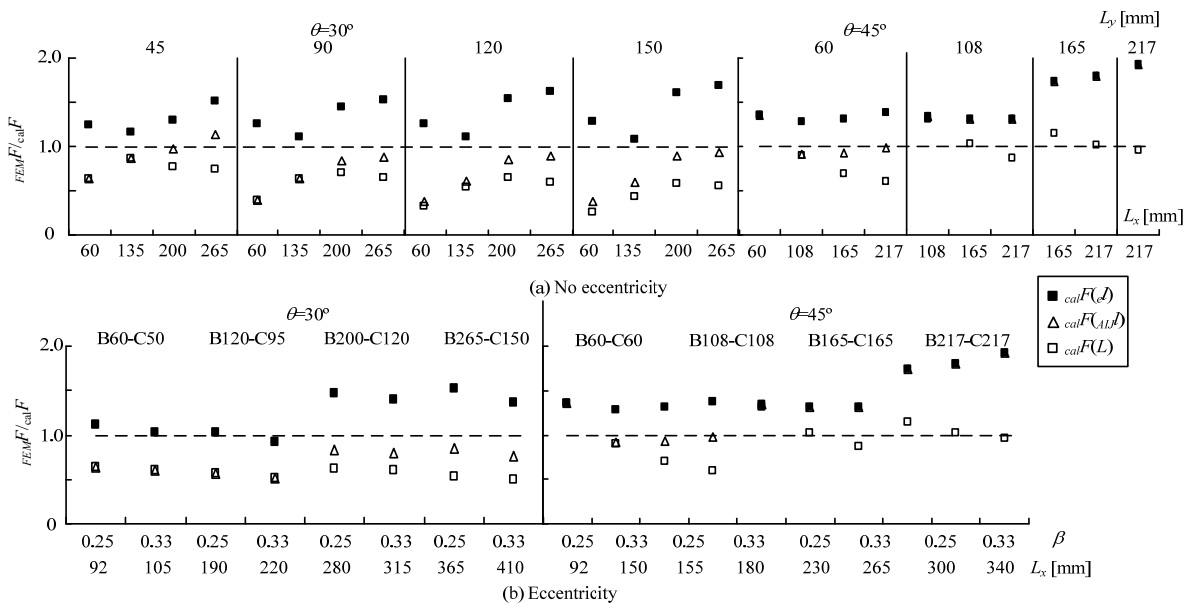


Figure 11. Comparison of ultimate strength of interface calculated by using three different effective length.